NASA TECHNICAL MEMORANDUM

NASA TM X-68214

NASA TM X-68214

SELF-ACTING AND HYDRODYNAMIC SHAFT SEALS

by Lawrence P. Ludwig
Lewis Research Center
Cleveland, Ohio 44135

TECHNICAL PAPER proposed for presentation at
Seal Education Course of the Annual Meeting of the
American Society of Lubrication Engineers
Chicago, Illinois, April 30-May 3, 1973

SELF-ACTING AND HYDRODYNAMIC SHAFT SEALS

by Lawrence P. Ludwig

National Aeronautics and Space Administration
Lewis Research Center
Cleveland, Ohio 44135

ABSTRACT

Self-acting and hydrodynamic seals are described. The analytical procedures are outlined for obtaining a seal force balance and the operating film thickness. Particular attention is given to primary ring response (seal vibration) to rotating seat face runout. This response analysis revealed three different vibration modes. Proposed applications of self-acting seals in gas turbine engines and in rocket vehicle turbopumps are described. Also experimental data on self-acting face seals operating under simulated gas turbine conditions are given; these data show the feasibility of operating the seal at conditions of 345 newtons per square centimeter (500 psi) and 152 meters per second (500 ft/sec) sliding speed.

E-7406

INTRODUCTION

Considerable effort has been put into development of self-acting and hydrodynamic seals because conventional contact seals cannot meet the ever increasing pressure, temperature and speed requirements of some modern and advanced rotating equipment. As an example, in advanced aircraft gas turbine operation, seal speeds are expected to reach 183 meters per second (600 ft/sec), and pressures may reach 345 newtons per square centimeter (500 psi) (ref. 1).

The present solution to severe operating conditions is to use clearance seals such as labyrinths; these seals are reliable but carry performance penalties because of high leakage.

In advanced industrial compressors, pressures to 3450 newtons per square centimeter (5000 psi) are under consideration. The current sealing system for these high pressures usually is a liquid buffer bushing that requires a high pressure pump and electric drive motor (also for fail-safe reasons a backup pump and motor is required). These compressor seal systems with their allied plumbing and controls take up considerable space and can cost as much as the compressor.

Thus, there is a need for reliable, low leakage shaft seals that require no external controls or equipment and that can operate at the pressures, temperatures and speeds of advanced machines. Recent studies

(refs. 2 and 3) demonstrated that the self-acting seals can operate at some of the advanced aircraft engine conditions and that they have much higher capability than conventional contact seals and much lower leakage than labyrinth seals. These types of seals may also have applications in industrial compressors.

The objectives of this work are to review the development of self-acting and hydrodynamic seals and to describe aerospace seal problem areas for which these seals have application. In particular the development of an aircraft gas turbine engine seal will be described in detail.

TERMINOLOGY

First a word about terminology. The terms "hydrodynamic" and "hydrostatic" are often applied to describe seals for compressible fluids as well as for incompressible fluids. But following the bearing terminology, the terms "self-acting" and "pneumostatic" will be used to describe seals for compressible fluids; and "hydrodynamic" and "hydrostatic" will be reserved for seals for incompressible fluids.

It should be noted that conventional contact seals often operate with separation of the sealing surfaces because of forces produced by self-acting, pneumostatic, hydrodynamic or hydrostatic effects. (These types of seals are not the subject of this paper). For example, many conventional radial face seals for liquids (such as water pump seals) run with hydrodynamic separation of the sealing surfaces; the hydrodynamic forces being produced by surface waviness caused by local thermal expansions and wear. Thus in a conventional radial face seal, the sealing and hydrodynamic bearing functions are performed by the same surfaces. This dual performance is speed limited, because the heat generated in shearing of the lubricating fluid film, causes fluid vaporization which degrades the hydrodynamic bearing action.

Data from reference 4, shown in figure 1, shows that oil boiling temperatures (539 K (510° F)) are readily achieved even under low speed shearing of a thin lubricating film of oil. In the case depicted (fig. 1), the sliding speed was 11.3 meters per second (37 ft/sec). (This result reveals why seal cooling and material conductivity are critical design parameters in high speed seals).

References 5 and 6 describe a radial face seal that operates hydrodynamically and, as a consequence, has much higher pressure and speed capability than conventional face seals. The construction of this hydrodynamic seal is similar to that of a conventional face seal except that the primary ring face contains circular grooves (see fig. 2). Seat rotation causes the sealed liquid to circulate through these grooves and thus the grooved region is cooler than the other regions. Therefore

thermal deformations produce wedge geometries that give rise to the hydrodynamic forces. Figure 2 also illustrates the hydrodynamic force (pressure profile) that is built up in the region of the circular grooves. This type of seal apparently maintains a more efficient hydrodynamic action (than a conventional face seal) as pressure and speeds increase, and thus it has superior performance. Successful operation at pressures to 2413 newtons per square centimeter (3500 psi) and 101 meters per second (333 ft/sec) for thousands of hours have been reported (refs. 5 and 6).

It should be noted that, as with conventional seals, the sealing and thrust bearing functions, of the seals described by references 5 and 6, are performed by the same surfaces. Since the surfaces do not contain any "machined in" bearing geometry this type of seal is not covered in this paper; although it, as with some conventional seals, operates hydrodynamically.

SELF-ACTING AND HYDRODYNAMIC SEALS

The subject of this paper is the type of self-acting and hydrodynamic seals in which the bearing and sealing functions are separated, the self-acting or hydrodynamic action being produced by a "machined in" bearing geometry and not by thermal distortion or wear. Figure 3 shows this type of self-acting seal. (Since a hydrodynamic seal assembly would be the same in principle, the discussion can be limited to the self-acting seal.)

Self-Acting Face Seal Nomenclature

A self-acting face seal is similar to a conventional face seal except for the added feature of a self-acting geometry (gas lubricated thrust bearing) as shown in figure 3 (ref. 7). As with a conventional face seal, it consists of a rotating seat that is attached to the shaft and a non-rotating primary ring assembly that moves in an axial direction; and, thus, the seal can accommodate axial motion such as engine thermal expansion. The secondary seal (piston ring) is subjected only to the axial motion (no rotation) of the primary ring assembly. Several springs provide mechanical force to maintain contact at start and stop. In operation, the sealing faces are separated a slight amount (in the range of 0.00025 to 0.00127 centimeters, (0.0001 to 0.0005 in.)) by action of the self-acting lift geometry. This positive separation results from the balance of seal forces and the gas film stiffness of the self-acting geometry. The self-acting geometry can be any of the various types used in gas thrust bearings; the Rayleigh step type is illustrated here.

Within the seal industry there is a wide variety of terms used to describe similar seal parts. The ASLE seal glossary (ref. 8) has provided much needed guidance in seal nomenclature, and the self-acting nomenclature that follows is mainly an extension of this ASLE work. The

nomenclature applying to an assembly of parts (fig. 3(a)) is:

1. Primary seal - Seal formed by the sealing faces of the seat and primary ring. Relative rotation occurs between these sealing faces.

2. Secondary seal - Seal formed by the sealing surfaces of the secondary ring. In the case of a bellows seal the secondary seal is the bellows itself.

3. Static seal - Seal formed by the mating surfaces of the primary ring and its carrier (in some designs the static seal is an interference fit).

4. Self-acting geometry (the term hydrodynamic geometry is used for incompressible fluids) - Lift-pad geometry (Rayleight step bearing) and mating face which together produce the thrust bearing action to separate the sealing surfaces.

5. Film thickness (h) - Distance between primary sealing faces or between surfaces forming the self-acting geometry. For parallel surfaces, the film thickness at the primary seal is the same as at the self-acting geometry. (Note that h may vary with radial and circumferential position and with time.)

6. Seal head - Assembly that is axially moveable and consisting of primary ring, its retainer (if any), and its carrier. (The retainer and the carrier are combined into one part in some designs.)

The nomenclature applying to single parts (fig. 3(a)) is:

1. Seat - Part having a primary sealing face and mechanically constrained with respect to axial motion.

2. Primary ring - Part having a primary sealing face and not constrained with respect to axial motion.

3. Retainer, primary ring - Part that retains primary ring.

4. Secondary ring - Part having secondary sealing surfaces which mate to the secondary sealing surfaces of the carriers.

Force Balance, General Description

To determine film thicknesses and leakage in a self-acting seal, the axial forces acting on the seal head (assembly of the primary ring and its carrier) must be determined for each operating condition. These forces are comprised of the self-acting lift force, the spring force, and the pneumatic force due to the sealed pressure. Essentially,

the analysis requires finding the film thickness for which the opening forces balance the closing forces. When this equilibrium film thickness is known, the leakage rate can be calculated. (It should be noted that this force balance procedure is for the case in which the seat face has zero runout with respect to the shaft centerline. Seat face runout introduces dynamic film thickness changes, as discussed in a later section.)

To illustrate force balance calculation, an aircraft gas turbine seal (ref. 9) was chosen as an example that is given in the following sections. The force balance analysis considers four design points (table I) namely: idle, takeoff, climb and cruise. The seal is a nominal 16.76 centimeter (6.6 in.) diameter size suitable for large gas turbine engines. Pertinent dimensions are given in figure 3.

ANALYSIS OF SELF-ACTING SEAL

Primary Seal Pressure Gradient (Opening Force)

In calculating the axial force balance of the primary ring, the pressure gradient in the primary seal must be considered (see fig. 3 for primary seal location). The quasi-one-dimensional flow model described in reference 10 was used for these calculations. From a gas leakage flow standpoint, the primary seal is a long passage. For example, a typical operating film thickness of a self-acting seal is in the range of 0.00102 centimeter (0.0004 in.), and a typical radial length of the primary seal is 0.127 centimeter (0.050 in.). Thus, the length-height ratio of the flow channel is 125/1. Previous work (refs. 11 and 12) has shown that this leakage passage has the following qualitative features:

1. Laminar leakage flow prevails over much of the range of interest in seals for gas turbines (pressure range of 345 N/cm^2 abs (500 psia)).

2. Sonic velocity (choking) exists at the passage exit when pressure ratios are approximately 4/1 or greater at a mean film thickness of 0.00102 centimeter (0.0004 in.).

3. Pressure profiles across the primary seal for choked and non-choked flow can be very different.

4. Since the primary seal radial width is small compared with its diameters, the area expansion effect on flow can be ignored.

5. The leakage flow and pressure profile are significantly different if the surfaces of the primary seal are not parallel. (See ref. 13 for a discussion of the effects of converging and diverging sealing surfaces.)

The primary seal and mathematical model used in the quasi-one-dimensional analysis of reference 10 is shown in figures 4 and 5. As

mentioned, the area expansion effects are ignored and the model is a passage of height h and length l.

From stagnation source conditions of P_o and V_o, see figure 5, an isentropic expansion is considered to occur ahead of the entrance to the primary seal gap. Thus, the entrance pressure, P_1, is less than the stagnation pressure P_o, and the entrance velocity, V_1, is a finite value. To account for entrance loss and viscous friction, it was found necessary to use an entrance loss coefficient of 0.6 (ref. 10). Thus, the entrance velocity, V_1, is less than that calculated by isentropic expansion.

Flow in the sealing gap is assumed one-dimensional and a friction factor is introduced to account for viscous losses. At the exit, three conditions are considered in the analysis. First, exit velocity V_2 is subsonic and exit pressure, P_2, is equal to reservoir pressure, P_3. Second, exit velocity, V_2, is sonic and exit pressure, P_2, is equal to reservoir pressure P_3, and third, exit velocity, V_2, is sonic, the flow is choked, and exit pressure, P_2, is greater than the reservoir pressure P_3. In addition, the following restrictions apply to the mathematical model (see ref. 10 for details):

1. Effect of seat rotation on flow is neglected.

2. For subsonic flow at a Mach number $\leq 1/(\text{specific-heat ratio})^{1/2}$, the flow is isothermal and the model yields the classical cubic dependence of mass flow on film thickness.

3. For flow at a Mach number $> 1/(\text{specific-heat ratio})^{1/2}$, the viscous effects are approximated by a mean friction factor of $24/Re_{2h}$ (Re = Reynolds number).

Typical pressure gradients across the primary seal for two design points (idle and take off) are shown in figure 6 (ref. 9). The important point is that choked and nonchoked flows can have pressure gradients with very different shapes thus affecting the opening force (that is, the integrated force under the pressure-gradient curves).

Figure 7 shows this primary seal opening force as a function of film thickness for the four design points. Note that for all four design points, the opening force is nearly independent of film thickness. (True only for parallel faces.)

Self-Acting Geometry (Opening Force)

The self-acting geometry (lift pads) consist of a series of shallow recesses 0.0025 centimeter (0.001 in.) deep arranged circumferentially around the seal under the primary seal face as shown in figures 8 and 9. An important point is that the lift pads are bounded at the inside diameter and the outside diameter by the sealed pressure P_1. (This is accomplished

by feed slots connecting the annular groove directly under the primary seal face.) Therefore, a pressure gradient due to gas leakage occurs only across the primary seal.

The complete primary ring and its 20 lift pads are shown in figure 9, and as indicated, motion of the seat over these shallow recesses drags air from the feed slots into the shallow pad recesses. Since the air is restricted from leaving the recesses by the side and back lands, a lift force, or thrust bearing action, is produced.

This self-acting lift pad is approximated by the mathematical model shown in figure 10. Note that the curvature effects have been neglected in the model. Therefore, the model corresponds to a Cartesian coordinate system. (The mathematical model is described in detail in reference 14.) In this analysis the following restrictions apply:

1. The fluid is Newtonian and viscous.

2. A laminar flow regime is assumed.

3. Body forces are negligible.

The analysis of reference 14 admits nonparallel surfaces; thus, the effects of surface deformation on lift force can be evaluated.

Figure 11 shows the calculated lift force (ref. 14) produced by the self-acting geometry for the four operating points of table I. Inspection of figure 11 reveals at film thicknesses of 0.00127 centimeter (0.0005 in.) and greater the lift force is small. However, at film thicknesses less than 0.00127 centimeters (0.0005 in.) the lift force rapidly increases as the film thickness decreases. Thus, the self-acting geometry has a very high film stiffness that enables the seal head to track the motions of the rotating seat face.

As mentioned previously, the self-acting lift force tends to open the seal, and is added to the primary seal opening force to obtain the total opening force. The resulting combined opening force given in figure 12. Again, this is for parallel surfaces only.

Closing Forces

The closing forces (see fig. 13) acting on the primary ring are a spring force and a pneumatic force. Since the full sealed pressure acts to the inside diameter of the primary seal, the net pneumatic closing force acts only on the annular area between the primary-seal inside diameter and the secondary-seal outside diameter. For the seal design under consideration this annular area is (see fig. 13):

$$A = \frac{\pi}{4}\left(D_1^2 - D_2^2\right) = 4.66 \text{ cm}^2 \ (0.722 \text{ in.}^2)$$

and the resulting closing forces due to the sealed pressure are listed in table II . It should be noted that these closing forces are for average dimensions at room temperature. At operating temperature, a thermal growth difference may cause a change in the relation between the secondary-seal outside diameter and the inside diameter of the primary seal. Thus, the closing force could be a function of temperature. However, in this report all force balance calculations are based on room-temperature dimensions. In critical applications the force balance at operating temperature may have to be evaluated.

Net Force Balance

In a conventional seal, the net closing force is resisted by solid-surface rubbing contact; thus, a total force balance is achieved. But in self-acting seals the force balance is achieved without rubbing contact. Therefore, for a given design point, the seal will operate at a film thickness such that the total opening force exactly balances the total closing force. This operating film thickness is obtained by plotting total opening forces (fig. 12) and total closing forces (table II) as a function of film thickness. The intersection (see fig. 14) of these curves is the equilibrium operating film thickness. This film thickness determination does not take into account dynamic running factors such as seat face runout and piston ring damping.

Once the equilibrium film thickness is found, the calculated leakage can be determined by using the quasi-one-dimensional method outlined in reference 10. For the four design points, this leakage rate is given in figure 15 for various film thicknesses, and table III shows the calculated leakage for the equilibrium film thicknesses of figure 14 (for parallel faces).

In designing a seal, each operating point should be checked for equilibrium film thickness. If these film thicknesses are not satisfactory, the closing force should be altered to bring all operating points within a satisfactory film thickness regime. Experience has shown that the satisfactory film thickness regime is about 0.00025 centimeter (0.0001 in.) on the low end (some tolerance to thermal deformation must be maintained) and 0.0013 centimeter (0.0005 in.) on the high end. These limits are only approximate and depend to a large extent on the dynamic and thermal condition to which the seal is subjected. The high limit of practical film thickness is established by seal dynamics and leakage considerations. In particular, the primary ring response to the seat face runout becomes excessive as the mean film thickness increases (ref. 15). This is because the stiffness of the gas film decreases with increasing film thickness. These dynamic considerations are covered in the section on face runout effects.

Effect of Nonparallel Seat Face

Figure 16 shows, in an exaggerated manner, the coning displacement of the seal seat. (The primary ring could also be coned.) This type of coning displacement, which can be caused by thermal gradients, results in nonparallel faces within the primary seal and the self-acting geometry. These nonparallel faces have a significant effect on load capacity of the self-acting geometry; also the primary seal opening force is affected. Thus, in design, the equilibrium operating film thickness should also be calculated for anticipated coning displacements.

As an example of the effect of this coning, design point 2 was checked (using the methods of reference 14) for equilibrium film thickness for a distortion of 0.0013 centimeter (0.0005 in.) across the self-acting pad. This is a distortion of 2 milliradians and is judged typical of some seal operation (ref. 15). Figure 17 shows this assumed distortion in an exaggerated manner; note that the self-acting geometry and primary seal dimensions are given.

Figure 18 shows the self-acting lift force for the 2-milliradian distortion of the seat face. Note that the force is plotted as a function of the mean film thickness of the self-acting pad. Also plotted, for comparison, is force generated for a parallel film. Note the significant reduction in lift force due to distortion, especially at the lower film thicknesses.

As noted previously, the primary seal opening force is also affected by nonparallel faces; and this was calculated by using an analysis similar to reference 12 for the 2-milliradian distortion. The results are given in figure 19. For the divergent deformation shown in figure 17, there is a marked reduction in opening force as the film thickness decreases. For convergent deformation, the opening force would increase as film thickness decreases; and this is desirable. Unfortunately, in aircraft mainshaft seals, the divergent deformation is a natural tendency due to thermal gradients.

Finally, in figure 20, the equilibrium film thickness for a 2 milliradian distortion is found by finding the intersection between the total closing force and total opening force. The mean film thickness is about 0.00169 centimeters (0.00066 in.). Thus the minimum film thickness is 0.00104 centimeters (0.00041).

With the equilibrium film thickness values, the gas leakage was calculated by using the method previously outlined. The results revealed that the leakage rate for the 2-milliradian deformation was nearly twice that of the parallel-face case.

Effect of Seat Face Runout

The preceding analysis was for operating film thicknesses that did not vary with time and this would be the situation if the rotating seat face had zero runout. However, the seat face will always have some runout with respect to the axis of rotation; and in particular, the maximum runout used in practice is of interest since it will induce the maximum time-dependent film thickness changes.

Of interest, then, is how the primary ring responds to the runout motions of the seat face. This response determines the film thicknesses at any instant. Experimental data reported in reference 15 reveal that the primary ring can follow (dynamically track) the seat face motion over a considerable range of face runouts. This data was obtained by mounting two proximity probes (90° apart) on the ring retainer and recording the change in film thickness as a function of time. A schematic showing the probe location is given in figure 21. Some results from reference 15 are given in figure 22 which shows that for a seat face runout of 0.0020 centimeter (0.00085 in.) full-indicator reading (F.I.R) the ring response is nearly in phase and the total change in film thickness is 0.0017 centimeters (0.00067 in.).

Also, the film thickness varies circumferentially; that is, the film thickness is not axisymmetric. This response of the primary ring can be explained by observing the time sequence at one point fixed with respect to the laboratory observer. This is shown in figure 23. The upper part of figure 23 illustrates seat and primary ring with maximum film thickness (exaggerated) at a time arbitrarily designated as zero. At some later time, when the seat has rotated thru 180°, the film thickness at this point is a minimum. Figure 2B could also represent the simultaneous film thicknesses 180° apart.

An analytical program has been developed for the purpose of predicting this ring response to seat face runout (ref. 16). Analysis of the seal depicted in figure 3 revealed that the primary ring response is markedly affected by secondary seal friction and by inertia of the primary ring assembly. The friction effect is illustrated in figure 24; as runout increases, there is a friction level that, if exceeded, will retard the primary ring motion to such an extent that rubbing contact will occur (line (1)); also for the higher face runouts there is a friction level below which the inertia forces are so high that the primary ring cannot follow the runout (line (2)). Therefore, some friction is probably desirable for most applications because of the practical limits on control of face runouts. Further, the data suggest that the primary ring assembly inertia should be kept as small as practical in order to maintain good response (avoid unstable operation). Figure 24 in general shows only how the nosepiece response is affected by secondary seal friction and seat face runout; in a detailed analysis by reference 17,

three different types of nosepiece responses were revealed by a parametric study using different magnitudes of seat face runout and secondary seal friction. These three cases are:

Case 1 - primary ring motion duplicates seat face runout motion and can be described by rotation (rocking) about two orthogonal axes. However, because of primary ring inertia and/or friction, the face of the ring has an angular misalinement with respect to the face of the seat. Therefore, the film thickness between the faces is not uniform.

Case 2 - Same as case one plus an additional axial vibration component.

Case 3 - Seal failure (film thickness reaches zero). This case can occur when the frictional forces are either too low (when inertia forces are high) or too high for the available load capacity of the self-acting pads.

Results from reference 17 predict case 2 type operation for the seal shown in figure 3. These results are shown in figures 25 to 27. The primary ring assembly weight is 0.80 kilograms (1.75 lbw), and other operating conditions (which simulate operation in a gas turbine) are:

Sealed pressure, newtons per square centimeter.	207 (300 psi)
Sealed gas temperature, K	811 (1000° F)
Sliding speed, meters per second.	152 (500 ft/sec)
Initial film thickness, centimeters	0.00081 (0.00032 in.)

Figure 25 shows the rotation (rocking) about the X-axis (motion about the Y-axis is the same except for a 90° phase shift). The trace indicates that rocking is not continuous with time, the ring "sticks" twice per revolution. This "sticking" also occurs in the motion about the Y-axis; therefore, a discontinuity in motion occurs four times per revolution. The effect of this discontinuity (four per revolution) is seen in the opening force of the self-acting geometry (figure 26). Each "sticking" leads to a decrease in film thickness and corresponding build-up of axial fluid film force. Thus the primary ring has a translation (axial) motion and this is shown in figure 27.

POTENTIAL APPLICATIONS

Gas Turbine Mainshaft Seals

Mainshaft seals are used in gas turbine engines to restrict gas leakage into the bearing compartments (sumps). The seal at the front of the compressor (fig. 28) usually presents no problem since the sump can be surrounded by compressor bleed air of moderate pressure and

temperature. Bleed air leaks through the seal and, thus, pressurizes the sump. For moderate bleed air pressures and temperatures, almost any type of seal is adequate (ring, circumferential, or face type). As an example, ring seals have been used at 37.2 newtons per square centimeter (54 psi) and 438 K (330° F). Circumferential seals have been used to 58.6 newtons per square centimeter (85 psi) and 644 K (700° F) with a sliding speed of 73.2 meters per second (240 feet per second). Face seals are also adequate, as some are operating at 86 newtons per square centimeter (125 psi), 700K (800° F), and a sliding speed of 107 meters per second (350 feet per second). (The final selection of the seal type for the front compressor location depends on the many design and system considerations, including designer preference.

The seal operational requirements become more severe at the middle of the engine and at the turbine bearing sump. The thrust bearing must be large enough to carry the net thrust load of the rotating parts. In addition, the sump is usually surrounded by higher pressure gas, and corresponding higher temperature, than the front of the engine.

Some shaft seal arrangements for the turbine bearing sump location are shown in figures 29 to 31. Here the basic problem is protection of the bearing sump from the turbine cooling gas. In early engines, since the cooling gas pressure and temperature were relatively low, a single labyrinth seal, which restricted turbine cooling gas leakage into the sump, was adequate (fig. 29). (Some engines use a once-through lubrication system in which the sump is pressurized by relatively cool bleed air, and this air and the oil lubricant are allowed to vent overboard.) At these pressures, the efficiency loss (and oil loss) due to seal leakage was not significant.

A disadvantage of the labyrinth seal, as compared to the close-clearance seals (ring, circumferential, and face), is high leakage with corresponding larger ducting requirements and easier passage of airborne water and dirt into the sump. In addition, for labyrinth seals, reverse pressure drops must be avoided to preclude high oil loss. Furthermore, ram air temperature (minimum-temperature air available for sump-pressurizing) increases with increasing flight speed. Therefore, a flight speed limit exists beyond which the low-leakage close-clearance seals are desirable in order to preclude sump fires.

As turbine cooling gas pressure requirements increased with development of engines with higher turbine inlet pressures, the single labyrinth seal (fig. 29) was no longer suitable. A conventional face seal (fig. 30) has satisfactory performance to pressures of 86 newtons per square centimeter (125 psi), temperatures of 700 K (800° F), and sliding speeds of 107 meters per second (350 feet per second). Recent seal studies (ref. 2) showed that at higher pressures, temperatures, or sliding speeds performance was unsatisfactory from a wear and leakage standpoint; subsequent analysis revealed that the seal limitations were primarily due to thermal

deformations that induced seal imbalance, which, in turn, caused high wear and leakage.

When the pressure, speed, and temperatures exceed the capability of conventional contact seals (such as that of fig. 30), a pressure staging seal system of multi-labyrinths is used (such as that in figure 31). In this seal system, a labyrinth seal restricts the leakage of relatively high pressure (P_1), high-temperature turbine cooling gas to an overboard vent or to a low-pressure region (P_0'). Low-pressure compressor bleed (P_1') surrounds the sump and, hence, provides thermal protection; and leakage (through the labyrinth) into the sump provides required sump pressurization. It should be noted that, as the turbine cooling gas pressure (P_1) increases, the labyrinth seal leakage increases and the detrimental effect on efficiency increases. For example in some modern engines the loss in thrust specific fuel consumption amounts to 0.9 percent at one seal location.

It is anticipated that advanced engines will have compressor discharge pressures in the range of 276 to 345 newtons per square centimeter (400 to 500 psi) and seal temperatures of approximately 1033 K (1400° F). The seals for these engines will have sliding speeds of 152 to 183 meters per second (500 to 600 feet per second). Engines for supersonic aircraft may generally have lower compressor discharge pressures, but the turbine cooling gas temperatures will be near 922 K (1200° F). The high sliding speeds in these advanced engines dictate that the sealing surfaces should not be in rubbing contact. Thus, the self-acting seals, since they operate without rubbing contact, are potentially useful in the advanced engines.

Simulated Gas Turbine Engine Operation

The self-acting face seal (fig. 3) was evaluated under conditions that simulated the environment of a gas turbine engine sump over a wide range of combinations of oil temperature, seal sliding speed, sealed pressure differential, and sealed air temperature (ref. 3). The rig used is shown in a cross-sectional view in figure 32. The rig shaft was mounted on a 130-millimeter-bore roller bearing and on a 110-millimeter-bore duplex ball bearing that carried the thrust from the sealed pressure; both bearings are typical of those used in large aircraft engines. The air to be sealed (maximum of 922 K (1200° F) and 345 newtons per square centimeter (500 psi)) is introduced through tubes as shown in figure 32. Thus, the sealed pressure is at the inside diameter of the primary ring, and air leakage is across the primary sealing faces (dam) into the bearing sump (also see fig. 3). Air also leaks across the secondary sealing surfaces into the sump.

The test rig is driven by an industrial internal combustion engine driving through a four-speed truck transmission and 12:1 step-up gear

box (fig. 33). The operating speed range was 7000 to 21 000 rpm. Oil was supplied to the rig bearing at temperatures typical of engine sumps (394 K (250° F) to 450 K (350° F)). The sealed air is heated to operating temperature by a resistance heater. In the later runs, a 25-micrometer filter was introduced (shown dashed in fig. 33) for the purpose of reducing the amount of hard particles carried by the air leakage flow. (The hard particles were found to be oxides generated in the resistance heater.)

A general increase in air leakage was noted as speed increased. This means that the average gas film thickness between the sealing surfaces increased as the speed increased. This result was attributed to primary ring response as discussed in the section on face runout and secondary seal friction effects.

To check wear and leakage characteristics the seal was subjected to long term runs (10 to 300 hours). A typical example of seal leakage is shown in figure 34 for a 100-hour run at a sliding speed of 122 meters per second (400 ft/sec), a sealed pressure differential of 138 newtons per square centimeter (200 psi), and a gas temperature of 811 K (1000° F). From an initial seal leakage of 1.13 standard cubic meters per minute (40 scfm), the seal leakage decreased to 0.79 standard cubic meters per minute (28 scfm) at the end of the 100 hours. This gradual leakage decrease was attributed to wear-in of the secondary ring causing better sealing. (In some runs fretting wear of the secondary seal caused a gradual increase in seal leakage rate.)

Inspection after the 100 hour run (150 hours total time on the seal) revealed that the chromium-carbide-coated molybdenum seat was in excellent condition with no sign of severe contact between the seat and the seat ring nosepiece. The self-acting pad land surfaces were polished, and the primary ring sealing face (dam) had circumferential scratches indicating abrasion due to air entrained debris. (Probably hard particles from the air heater operating at 1144 K (1600° F).)

The abrasive effect of hard particles was checked in a separate 10 hour test run using crushed-quartz fed into the seal air at a rate of 3.6 grams per hour (0.125 oz/hr). The wear of the self-acting pads was insignificant and the sealing dam showed 31.75 micrometers (0.00125 in.) wear at the inner edge of the sealing dam.

In addition to the endurance test running, the seal was subjected to a wide range of operating conditions. No rubbing contact occurred under conditions as low as 69 newtons per square centimeter (100 psi) and 61 meters per second (200 ft/sec), to as high as 345 newtons per square centimeter (500 psi) and 152 meters per second (500 ft/sec). In addition, after 38 hours at pressures that ranged between 241 to 345 newtons per square centimeter (350 to 500 psi) and at sliding speeds between 122 to 183 meters per second (400 to 600 ft/sec) the primary ring

(carbon) wear was insignificant (see fig. 35). Typical leakage values are shown in table IV.

In order to check the effect of starting and stopping, the seal was subjected to 40 starts and stops with room-temperature air at 69 newtons per square centimeter (100 psi). The seal speed was increased from 0 to 76 meters per second (0 to 250 ft/sec) in about 15 seconds. The seal was then allowed to coast to a stop in about 25 seconds. A comparison of the surface profile traces before and after the 40 starts and stops revealed carbon wear to be less than 1.27 micrometers (0.00005 in.).

Rocket Engine Turbopump Applications

In rocket engine turbopumps, shaft seals are used to seal propellants such as liquid oxygen and hot hydrogen gas. Experience has shown that the shaft seal system is a very critical item and seal failure can result in total destruction of the vehicle. Figure 36 shows a typical rocket engine seal system used in current practice. The purpose of the system is to separate liquid oxygen at pressures as high as 310 newtons per square centimeter (450 psi) from the hot turbine gas at 689 newtons per square centimeter (1000 psi). The seal system consists of three sealing areas with a central helium purge and a dual vent.

The liquid oxygen seal is a conventional rubbing contact seal with a bellows secondary seal. Oxygen is prevented from leaking past the helium seal by the purge flow of helium, and both the oxygen and helium pass out the vent indicated in figure 36. A similar action occurs on the hot hydrogen gas side. However, the hydrogen gas seals are conventional ring (clearance) seals. The helium purge seals are also conventional ring (clearance) seals.

In the seal system such as depicted in figure 36 there are a number of problem areas, the most critical of which is compatibility of the seal material with liquid oxygen. Therefore, as indicated, welded bellows designs are very often used. Another problem area has been wear life. The typical wear life is now in the range of 2 to 3 hours, which is a satisfactory margin for the current rocket vehicles. However, for the shuttle vehicle a total life of 10 hours is needed with a start-stop (mission) capability of 100. Clearly, the current seal technology is not adequate for the shuttle life requirements; and the self-acting seal may provide a solution.

An advanced seal system is under development (fig. 37) with a hydrodynamic seal for liquid oxygen and a self-acting circumferential seal for the helium. The seal for liquid oxygen is a hydrodynamic type with Regleigh step type thrust bearing geometry. Instead of a bellows secondary, a carbon piston ring is used. Liquid oxygen pressure is near

345 newtons per square centimeter (500 psi) and seal sliding speed about 137 meters per second (450 ft/sec). The predicted operating film thickness is 0.00076 centimeters (0.0003 in.).

The helium purge seal is a circumferential seal modified to have self-acting geometry similar to that shown in figure 38. This self-acting geometry, as in the case of the self-acting face seal, acts to maintain positive separation between the rotating shaft and the nonrotating carbon rings. The helium gas pressure is 35 to 69 newtons per square centimeter (50 to 100 psi). In comparison, the clearance ring seal shown in the conventional configuration (fig. 36) has a leakage rate 50 times greater. Thus, by use of the self-acting helium seals, the on-board helium inventory can be reduced and significant weight saving will acrue because of the smaller tanks and lines.

SUMMARY

Self-acting and hydrodynamic seals and their potential applications in gas turbine engines and in rocket engine turbopumps are described. In particular the analytical procedure is given for predicting the operating film thickness of a 16.76 centimeter (6.6 in.) diameter seal designed for gas turbine applications. The analysis and subsequent operation of this seal under simulated gas turbine conditions revealed the following:

1. Analysis

a. Noncontact operation with acceptable leakage is predicted at the selected four design conditions of idle, takeoff, climb, and cruise.

b. The operating film thickness ranged between 0.00046 and 0.00119 centimeter (0.00018 and 0.00047 in.) for the four design conditions.

c. The calculated seal leakage rates ranged between 0.01 and 0.40 scmm (0.4 and 14.0 scfm) for the four design conditions.

d. For a typical operating condition, noncontact operation was predicted under the assumption of a 2-milliradian face deformation. Gas leakage was about twice that for parallel-face operation.

2. Experiment-Simulated Engine Operation

a. The self-acting seal ran without rubbing contact during all of the simulated engine operating conditions. Of particular interest was that noncontact operation was maintained at the advanced engine conditions of a 152-meter-per-second (500 ft/sec) sliding speed, a 345 newtons per square centimeter (500 psi) sealed pressure differential, and a 811 K (1000° F) sealed air temperature.

b. The leakage rates during endurance tests ranged from 0.79 to 1.63 standard cubic meters per minute (28 to 57.5 scfm).

c. Self-acting geometry wear due to rubbing contact proved to be insignificant.

d. Two seal wear problems were noted. These are (1) fretting wear of the secondary ring (piston ring) and (2) erosion of the seal dam (primary seal) by hard particles.

e. Wear due to starts and stops proved to be insignificant. For 40 starts and stops wear was less than 1.27 micrometers (0.00005 in.).

REFERENCES

1. Anon., "Aircraft Propulsion," NASA SP-259 (1971).

2. Parks, A. J., McKibbin, R. H., Ng, C. C. W., and Slayton, R. M., "Development of Main-shaft Seals for Advanced Air Breathing Propulsion Systems," Pratt & Whitney Aircraft Rep. PWA-3161, NASA CR-72338 (1967).

3. Povinelli, V. P., and McKibbin, A. H., "Development of Mainshaft Seals for Advanced Air Breathing Propulsion Systems - Phase II," Pratt & Whitney Aircraft Rep. PWA-3933, NASA CR-72737 (1970).

4. Orcutt, F. K., "An Investigation of the Operation and Failure of Mechanical Face Seals," Presented at the 4th International Conference on Fluid Sealing, British Hydromechanics Research Association, Cranfield, Bedford, England (1969).

5. Mayer, E., "High Duty Mechanical Seals for Nuclear Power Stations," Paper A5, Presented at the 5th International Conference on Fluid Sealing, British Hydromechanics Research Association, Cranfield, Bedford, England (1971).

6. Mayer, E., "Thermodynamics in Mechanical Seals," Presented at the 4th International Conference on Fluid Sealing, British Hydromechanics Research Association, Cranfield, Bedford, England (1969).

7. Ludwig, L. P., and Johnson, R. L., "Design Study of Shaft Face Seal with Self-Acting Lift Augmentation. III - Mechanical Components," NASA TN D-6164 (1971).

8. Brown, P. F., "A Glossary of Seal Terms," Special Publication SP-1, American Society of Lubrication Engineers.

9. Ludwig, L. P., Zuk, J., and Johnson, R. L., "Design Study of Shaft Face Seal with Self-Acting Lift Augmentation. IV - Force Balance," NASA TN D-6568 (1972).

10. Zuk, J., Ludwig, P., and Johnson, R. L., "Quasi-One-Dimensional Compressible Flow Across Face Seals and Narrow Slots. I - Analysis," NASA TN D-6668 (1972).

11. Zuk, J., and Ludwig, L. P., "Investigation of Isothermal, Compressible Flow Across a Rotating Sealing Dam. I - Analysis," NASA TN D-5344 (1969).

12. Zuk, J., and Smith, P. J., "Computer Program for Viscous Isothermal Compressible Flow Across a Sealing Dam with Small Tilt Angle," NASA TN D-5373 (1969).

13. Johnson, R. L., and Ludwig, L. P., "Shaft Face Seal with Self-Acting Lift Augmentation for Advanced Gas Turbine Engines," NASA TN D-5170 (1969).

14. Zuk, J., Ludwig, L. P., and Johnson, R. L., "Design Study of Shaft Face Seal with Self-Acting Lift Augmentation. I - Self-Acting Pad Geometry," NASA TN D-5744 (1970).

15. Hady, W. F., and Ludwig, L. P., "Experimental Investigation of Self-Acting-Lift-Pad Characteristics for Main-Shaft Seal Applications," NASA TN D-6384 (1971).

16. Colsher, R., and Shapiro, W., "Predicting Performance of Gas-Lubricated Seals Using Advanced Numerical Techniques," Franklin Inst. FIRL-I-C2429-4, AD-745333 (1972).

17. Colsher, R., and Shapiro, W., "Steady State and Dynamic Performance of Gas-Lubricated Seals," NASA CR-121093 in process.

TABLE I. - DESIGN POINTS

Design point	Sealed pressure, P_1		Sealed gas temperature		Seal sliding speed	
	N/cm^2 abs	psia	K	^oF	m/sec	ft/sec
1 - Idle	45	65	311	100	61	200
2 - Cruise	148	215	700	800	153	500
3 - Takeoff	217	315	977	1300	137	450
4 - Climb	148	215	811	1000	122	400

E-7406

TABLE II. - CLOSING FORCE

Design point	Pneumatic						Spring force, F_s		Total closing force, $F_t = F_p + F_s$	
	Sealed pressure, P_1		Pressure change, ΔP		Sealed-pressure closing force, F_p					
	N/cm^2 abs	psia	N/cm^2	psi	N	lbf	N	lbf	N	lbf
1 - Idle	45	65	34.5	50	160.6	36.1	71.2	16	231.7	52.1
2 - Cruise	148	215	138	200	641.0	144.1	↓	↓	711.1	160.1
3 - Takeoff	217	315	207	300	963.4	216.6			1034.6	232.6
4 - Climb	148	215	138	200	641.0	144.1			711.1	160.1

TABLE III. - EQUILIBRIUM FILM

THICKNESS AND GAS LEAKAGE

THROUGH PRIMARY SEAL

Design point	Equilibrium film thickness		Gas leakage	
	cm	in.	scmm	scfm
1 - Idle	0.0004	0.00018	0.008	0.3
2 - Cruise	.0011	.00044	.27	9.5
3 - Takeoff	.0012	.00047	.39	14.0
4 - Climb	.0010	.00040	.18	6.4

TABLE IV. - TEST CONDITIONS AND TYPICAL LEAKAGE RATES

Time		Sliding Speed		Seal Press		Air Temp		Air Leakage	
(Hrs.)	Total Hrs.	(m/sec)	(ft/sec)	(N/cm^2)	(psi)	(K)	(°F)	(scms x 10^3)	(scfm)
.5	.5	122	400	207	300	542	517	16.0	34.0
.5	1.0	122	400	275	400	616	650	19.8	42.0
.5	1.5	137	450	275	400	683	770	20.5	43.5
.5	2.0	153	500	275	400	709	816	20.5	43.5
1.0	3.0	168	550	275	400	742	876	20.3	43.0
1.5	4.5	153	500	275	400	714	825	20.1	42.5
.5	5.0	168	550	275	400	666	740	21.7	46.0
.25	5.25	168	550	310	450	639	690	24.8	52.5
.25	5.50	183	600	310	450	633	680	27.1	57.5

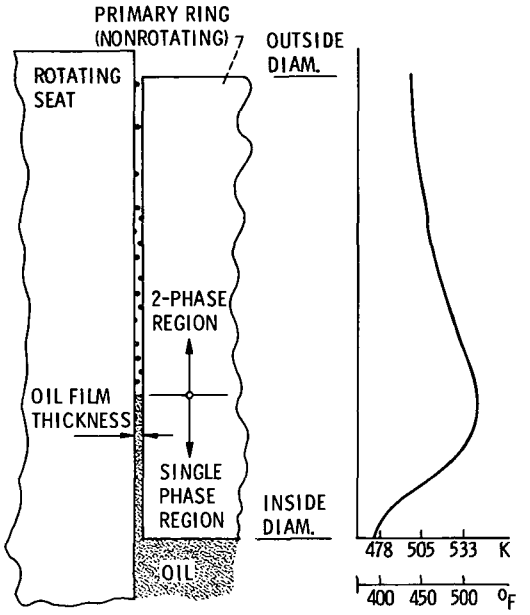

(a) SCHEMATIC OF OIL FILM IN PRIMARY SEAL.

(b) PRIMARY SEAL RADIAL TEMPERATURE PROFILE (DATA FROM REF. 4).

Figure 1. - Conventional oil lubricated radial face seal; seal siding speed, 11.3 meters per second (37 ft/sec).

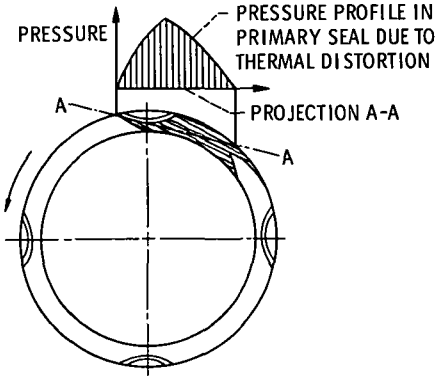

Figure 2. - Circular grooves in face of primary ring (from ref. 6).

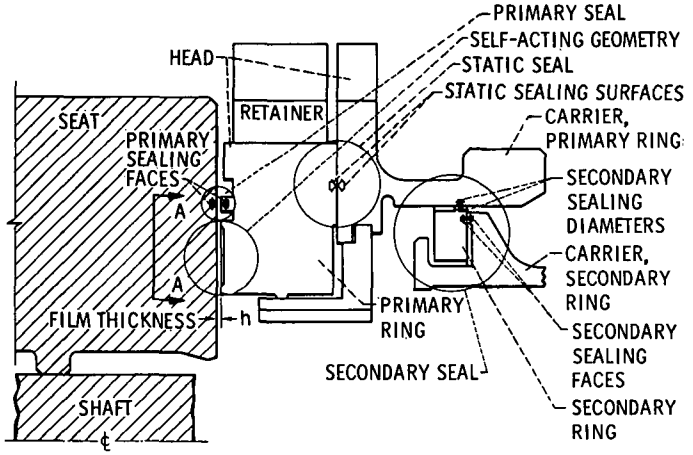

(a) NOMENCLATURE

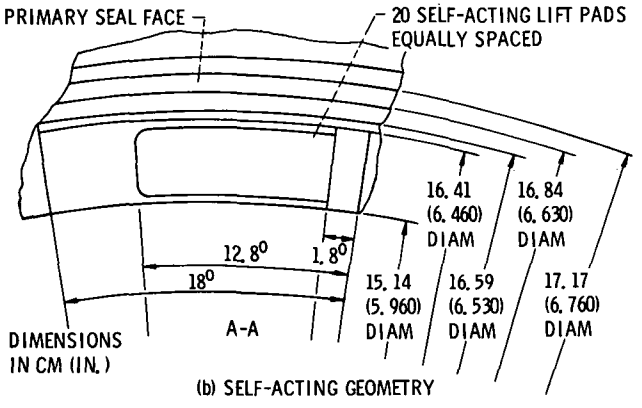

(b) SELF-ACTING GEOMETRY

Figure 3. - Self-acting face seal.

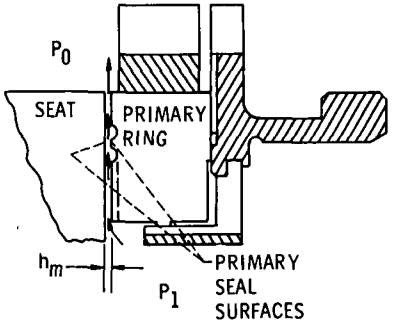

(a) PRIMARY SEAL LOCATION, $P_1 > P_0$.

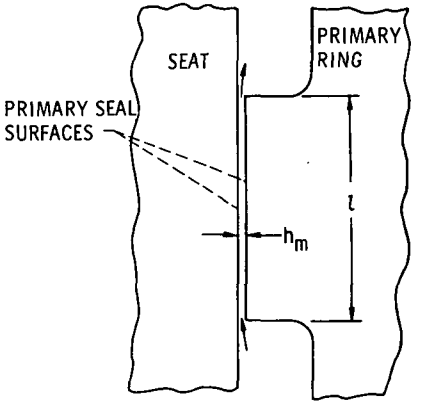

(b) EXAGGERATED VIEW OF PRIMARY SEAL.

Figure 4. - Primary seal.

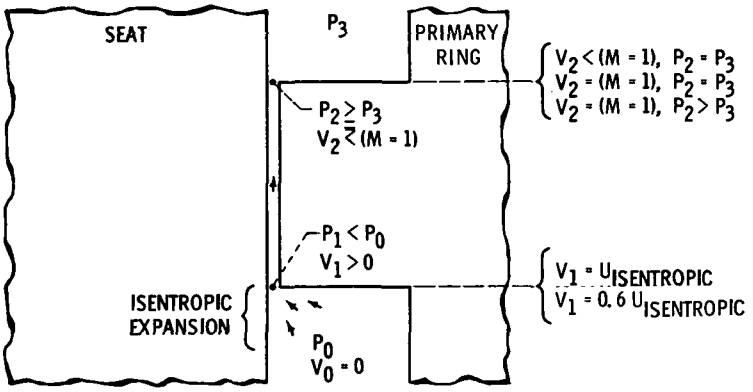

Figure 5. - Mathematical model of primary ring.

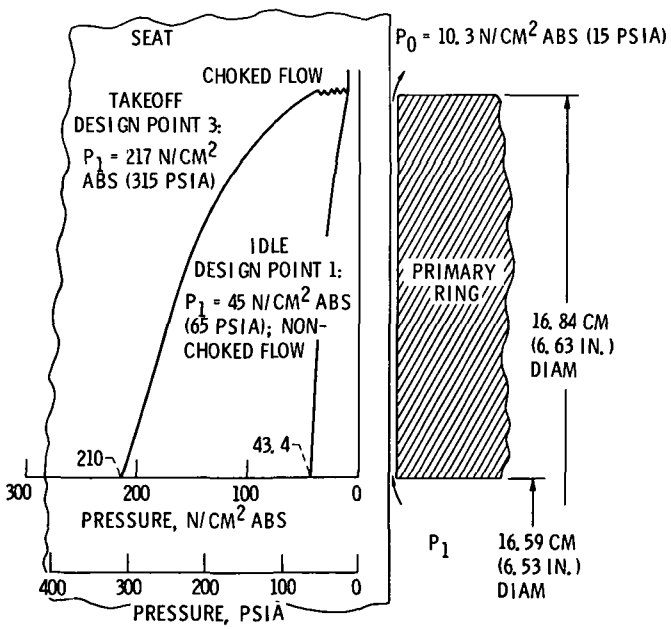

Figure 6. - Pressure gradient in primary seal, illustrating choked and nonchoked flow. Parallel face; mean film thickness h_m, 0.0010 centimeter (0.0004 in.). (From ref. 9.)

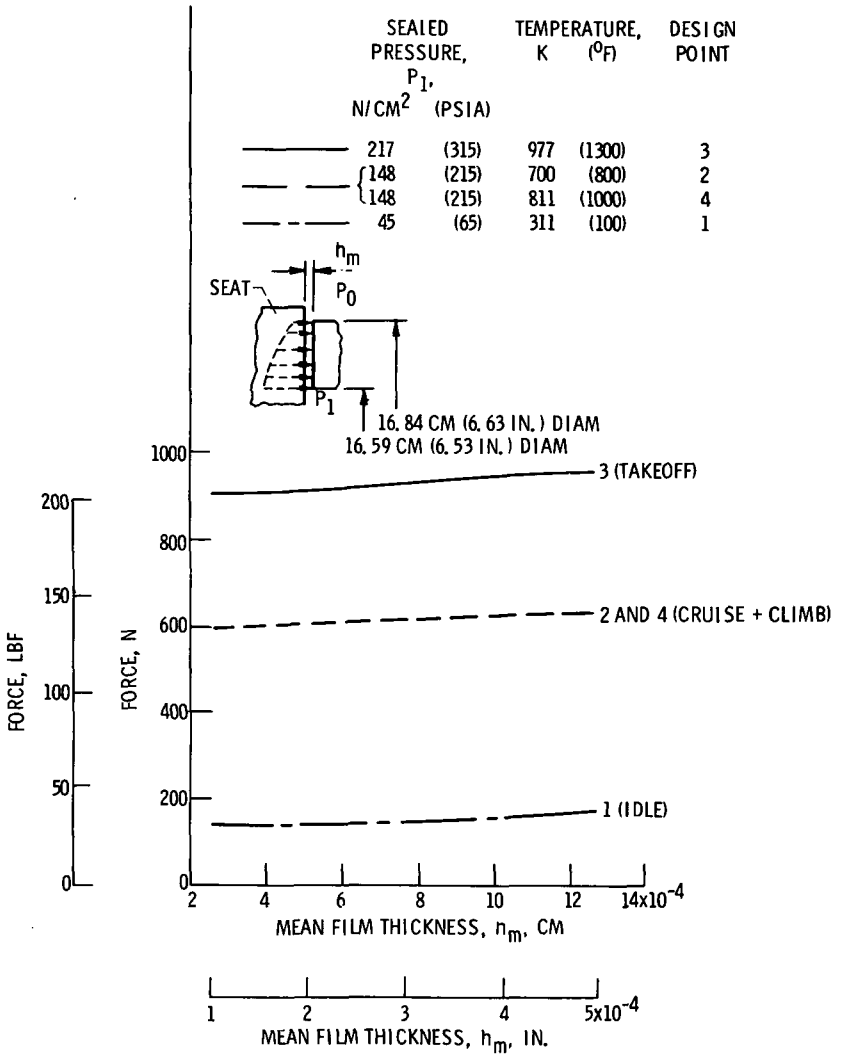

Figure 7. - Opening force acting on primary sealing face. fluid, air; sump pressure P_0, 10.3 N/cm^2 abs (15 psia); parallel faces.

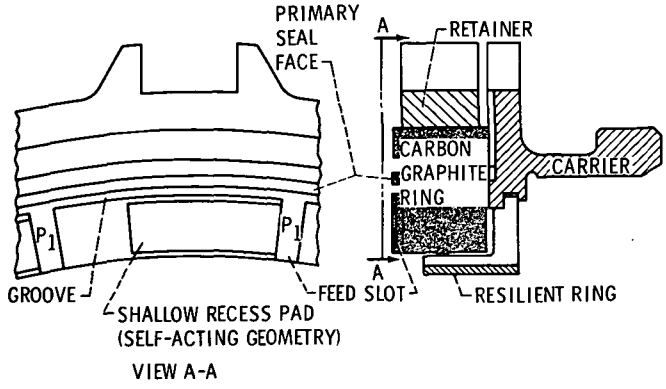

Figure 8. - Self-acting seal with pads on primary ring.

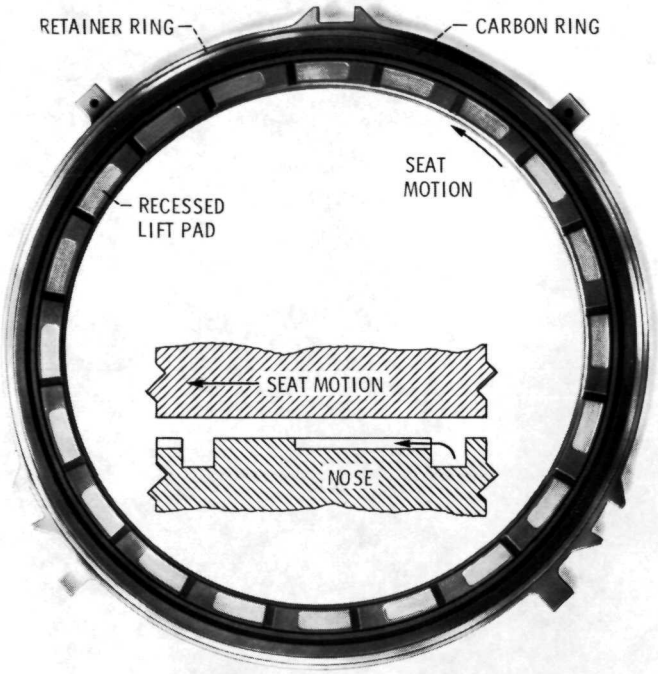

Figure 9. - Primary ring assembly.

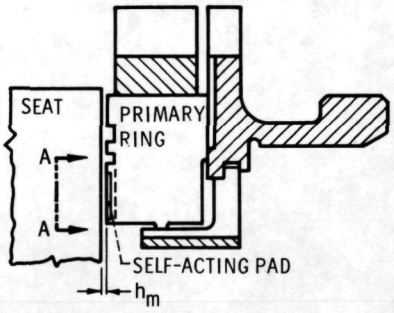

(a) SELF-ACTING PAD LOCATION.

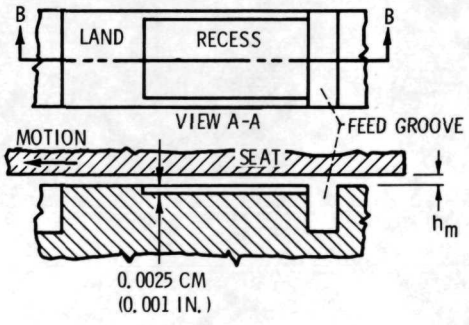

VIEW B-B

(b) MATHEMATICAL MODEL OF SELF-ACTING PAD WITH CURVATURE EFFECTS NEGLECTED

Figure 10. - Self-acting pad.

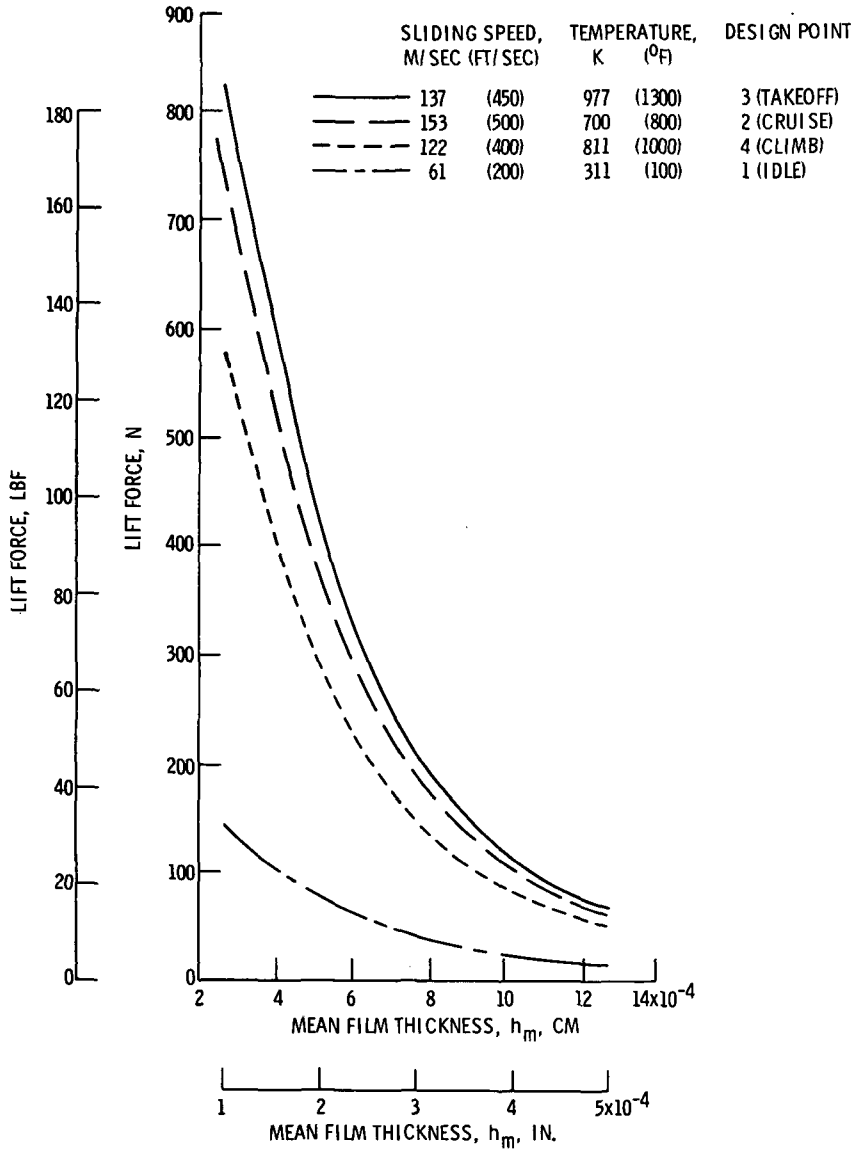

Figure 11. - Lift force of self-acting geometry. Number of pads, 20; recess depth, 0.0025 centimeter (0.001 in.); fluid, air; parallel faces. (From ref. 9.)

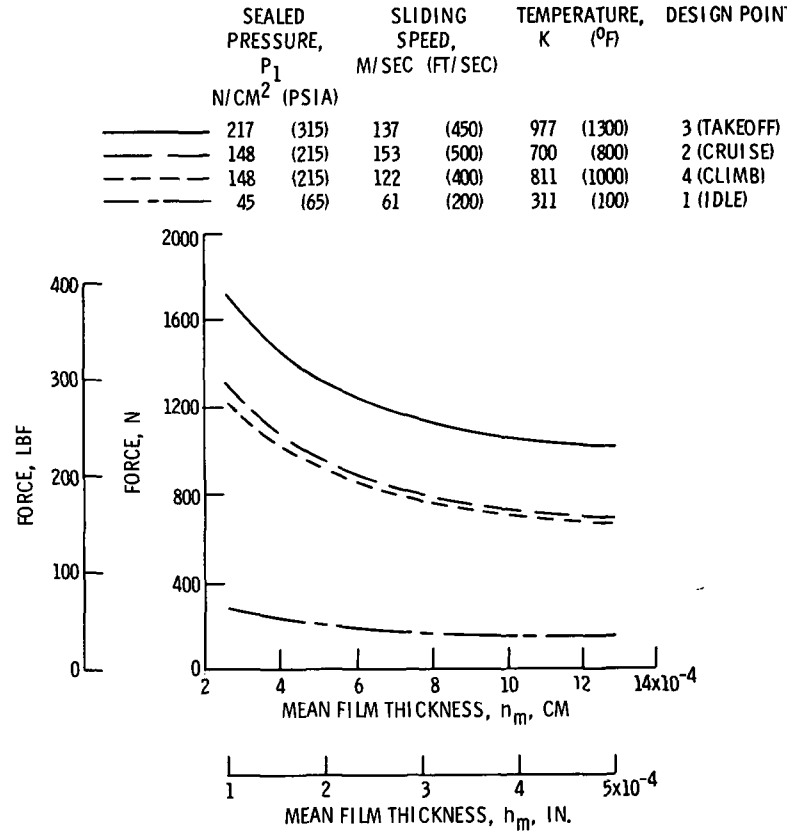

Figure 12. - Total opening force - self-acting pad lift force plus primary seal pneumatic force. (From ref. 9.)

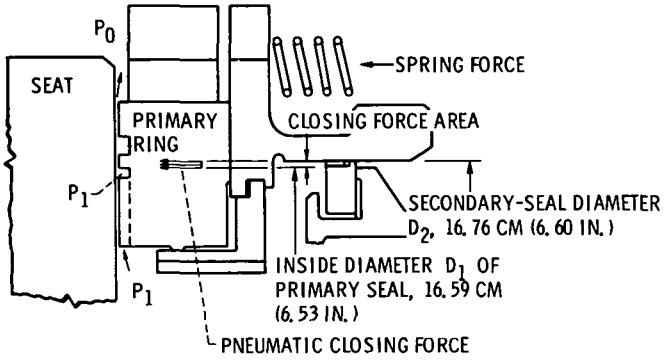

Figure 13. - Closing forces - spring force and net closing force due to sealed pressure.

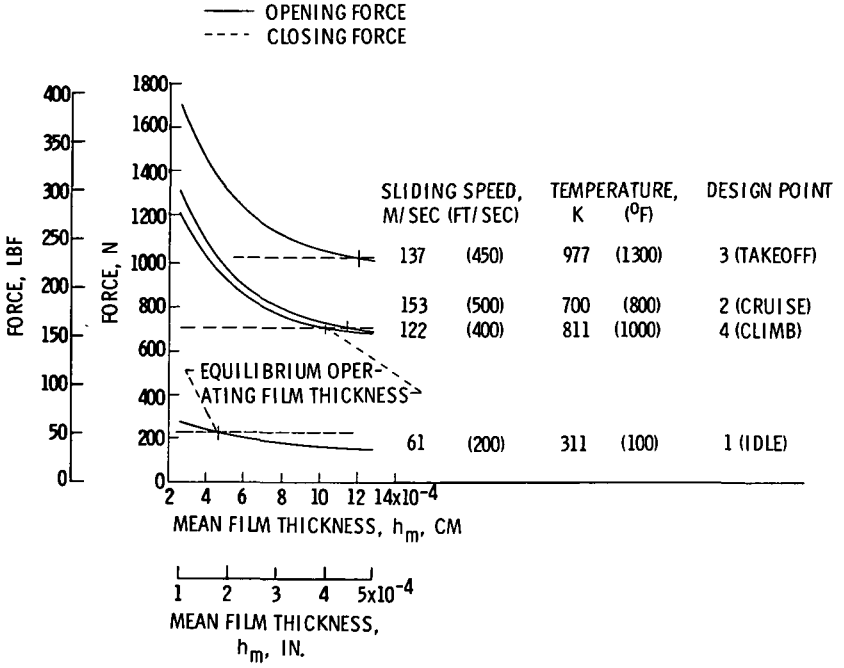

Figure 14. - Equilibrium gas film thickness as determined by total seal opening and closing forces. Parallel faces.

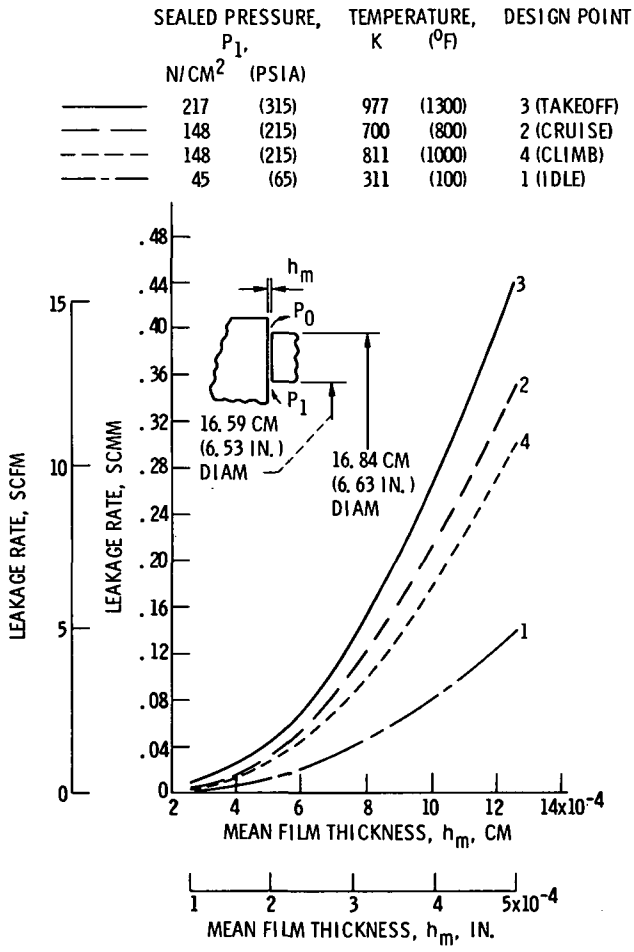

Figure 15. - Leakage rate as function of film thickness. Fluid, air; sump pressure P_0, 10.3 N/cm^2 abs (15 psia); parallel faces.

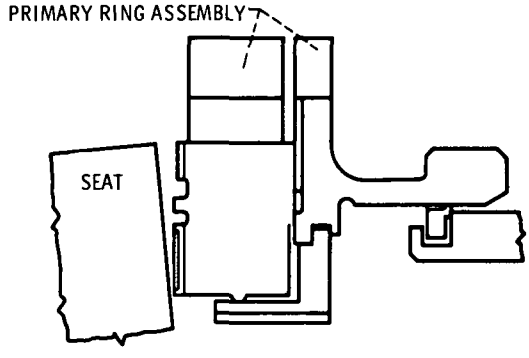

Figure 16. - Coning displacement of seat, causing non-parallel faces in primary seal and in self-acting geometry.

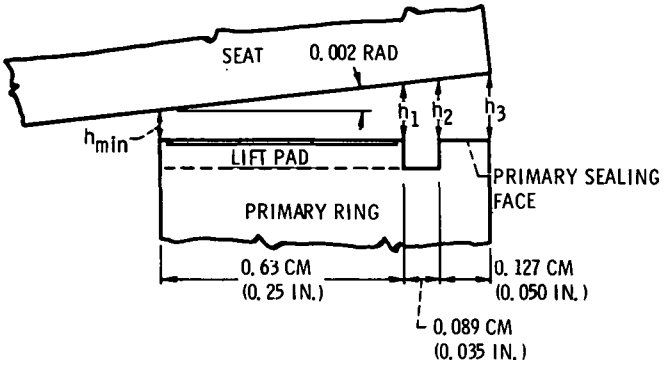

Figure 17. - Two-milliradian deformation of seal seat causing nonparallel faces in primary seal.

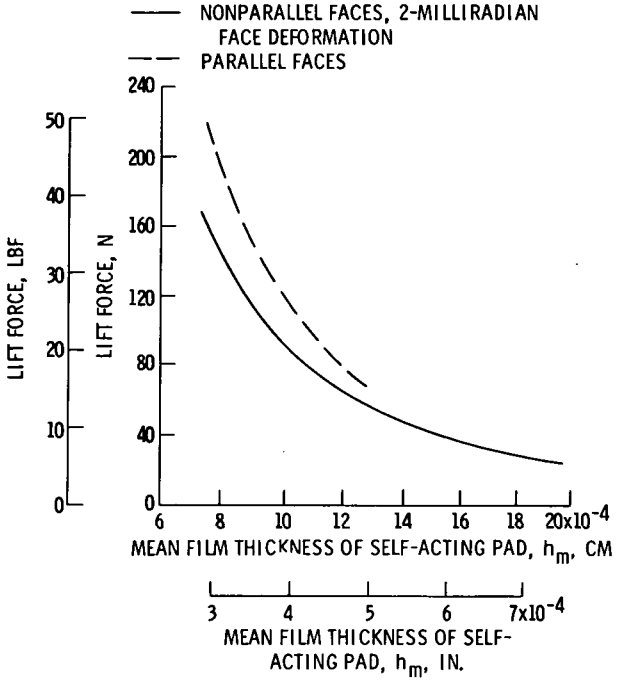

Figure 18. - Lift force of self-acting geometry. Number of pads, 20; pad depth, 0.0025 centimeter (0.001 in.); fluid, air. Design point 2; sealed pressure, 148 N/cm^2 abs (215 psia); sliding speed, 153 meters per second (500 ft/sec); fluid temperature, 700 K (800^0 F).

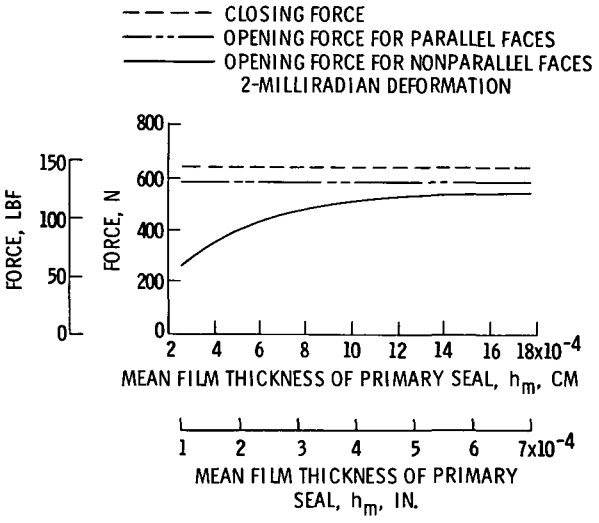

Figure 19. - Sealed pressure forces acting on primary ring assembly. Sealed fluid, air. Design point 2: sealed pressure, 148 N/cm^2 (215 psia); fluid temperature, 700 K (800^0 F). (From ref. 9.)

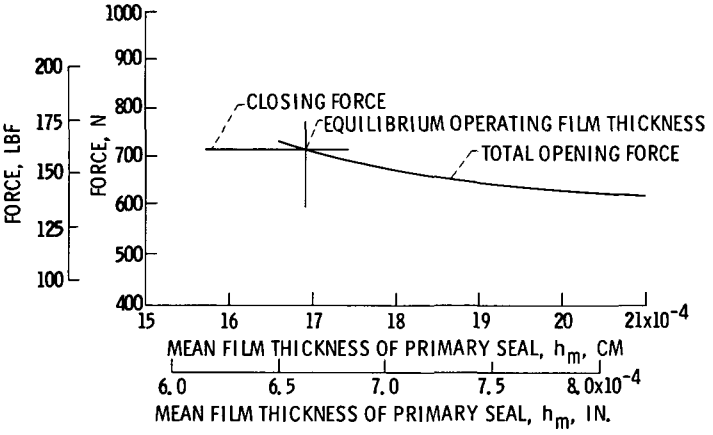

Figure 20. - Equilibrium gas film thickness as determined by total opening and closing forces for 2-milliradian face deformation. Design point 2: sliding speed, 153 meters per second (500 ft/sec); sealed pressure, 148 N/cm^2 abs (215 psia); sealed gas temperature, 700 K (1800^0 F).

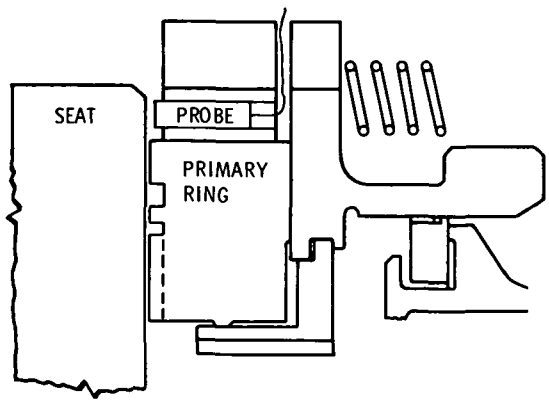

Figure 21. - Schematic showing priximity probe location.

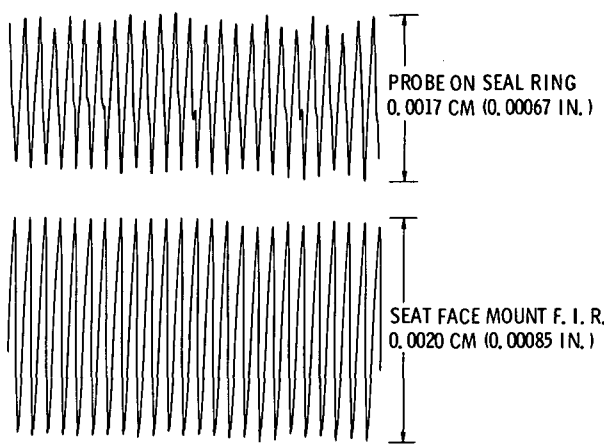

Figure 22. - Oscillograph traces showing response of ring to seat face runout. Recess-pad length to land-length ratio, 2:1; recess-pad depth, 0.0013 centimeter (0.0005 in.); sliding velocity, 61 meters per second (200 ft/sec); ambient pressure, 10 newtons per square centimeter (14.7 lb/in.^{2}); room temperature, 300 K (80^0 F); spring load, 1.13 kilograms (2.50 lb). (From ref. 15.)

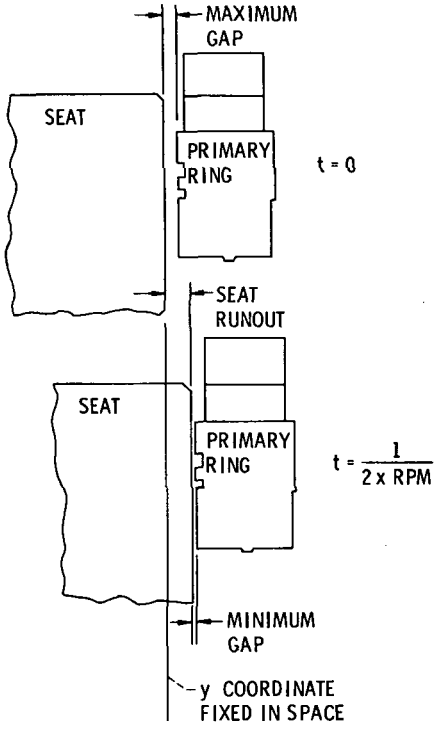

Figure 23. - Response of nose to seat face runout.

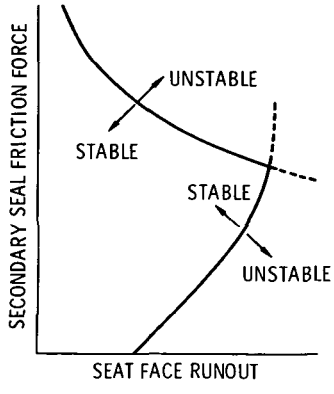

Figure 24. - Typical stability map of primary ring response to seat face runout.

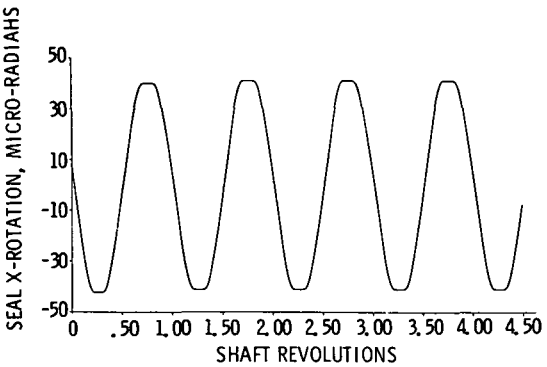

Figure 25. - Calculated rotation response of the primary ring; primary ring assembly weight, 0.78 kilogram (1.75 lbw); sealed gas pressure, 207 newtons per square centimeter (300 psi); sealed gas temperature, 811 K (1000° F); sliding speed, 152 meters per second (500 ft/sec); initial film thickness, 0.00081 centimeter (0.00032 in.); seat face runout 0.00635 centimeter (0.0025 in.) full indicator reading.

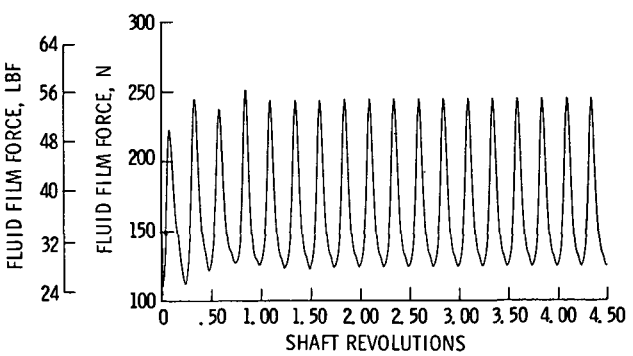

Figure 26. - Calculated fluid film force of the self-acting geometry; primary ring assembly weight, 0.78 kilogram (1.75 lbw); sealed gas pressure, 207 newtons per square centimeter (300 psi); sealed gas temperature, 811 K (1000° F); seal sliding speed, 152 meters per second (500 ft/sec); initial film thickness, 0.00081 centimeter (0.00032 in.); seat face runout 0.00635 centimeter (0.0025 in.) full indicator reading.

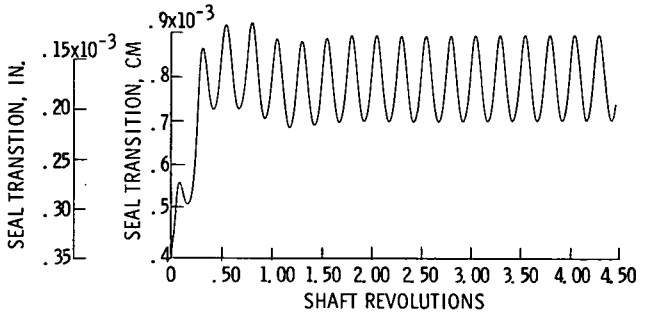

Figure 27. - Calculated translation motion of the primary ring assembly; primary ring assembly weight, 0.78 kilograms (1.75 lbw); seal gas pressure, 207 newtons per square centimeter (300 psi); sealed gas temperature, 811 K (1000° F); seal sliding speed, 152 meters per second (500 ft/sec); initial film thickness, 0.00081 centimeter (0.00032 in.); seat face runout, 0.00635 centimeter (0.0025 in.) full indicator reading.

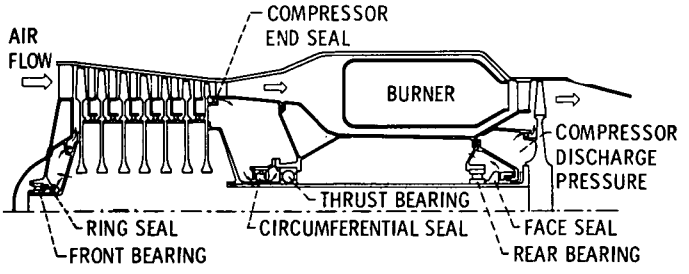

Figure 28. - Schematic of engine showing typical seal locations.

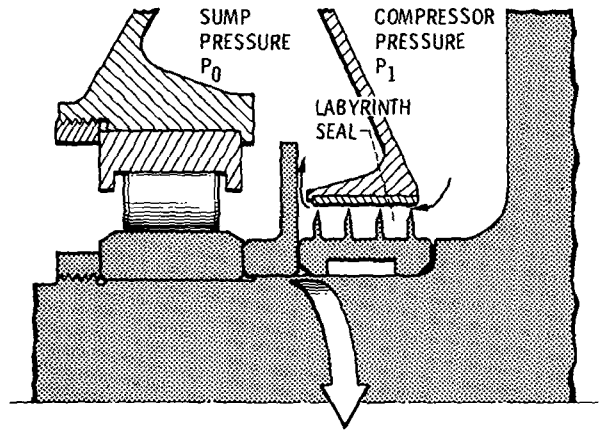

Figure 29. - Single labyrinth seal - early engine or low pressure designs.

E-7406

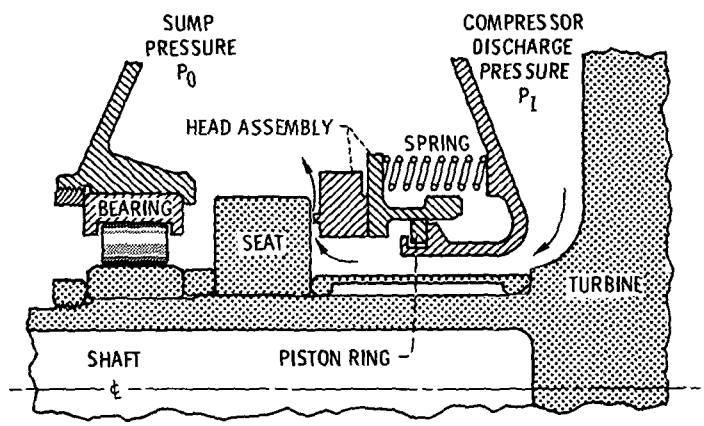

Figure 30. - Schematic of a conventional radial face main shaft seal.

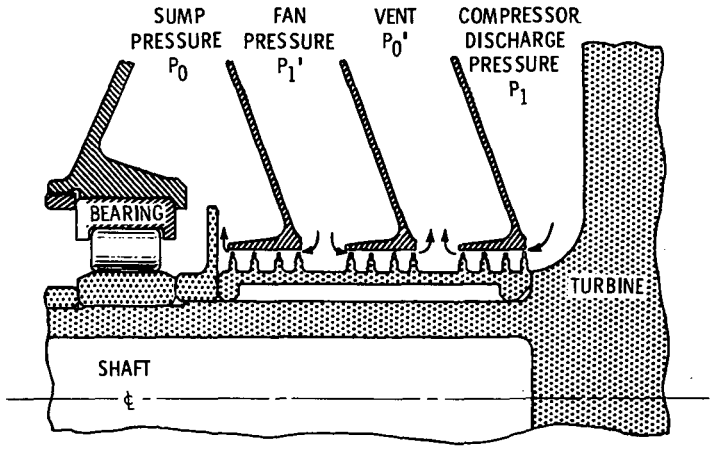

Figure 31. - Labyrinth seal system schematic.

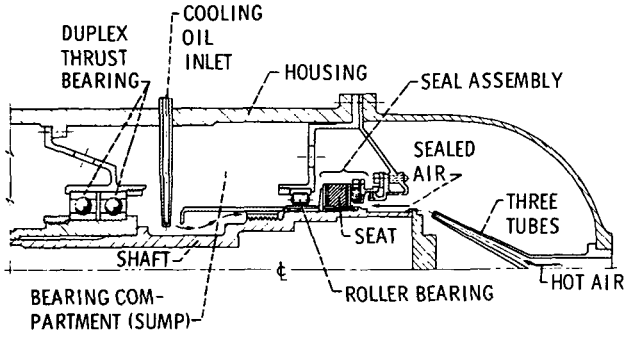

Figure 32. - Rig used for experimental evaluation of seals.

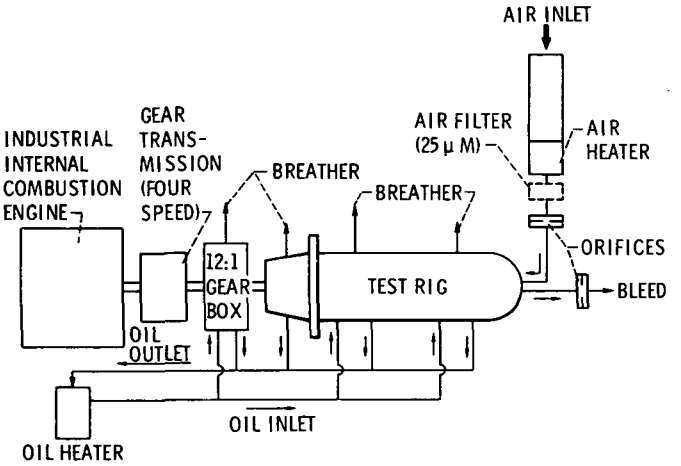

Figure 33. - Test facilities.

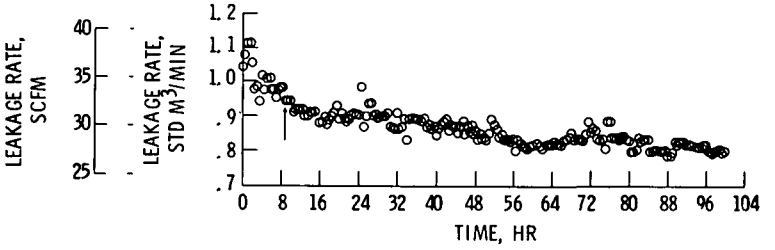

Figure 34. - Air leakage self-acting seal during 100-hour endurance run. Seal sliding speed, 122 meters per second (400 ft/sec); sealed pressure differential, 138 N/cm^2 (200 psi); sealed gas temperature, 811 K (1000^0 F).

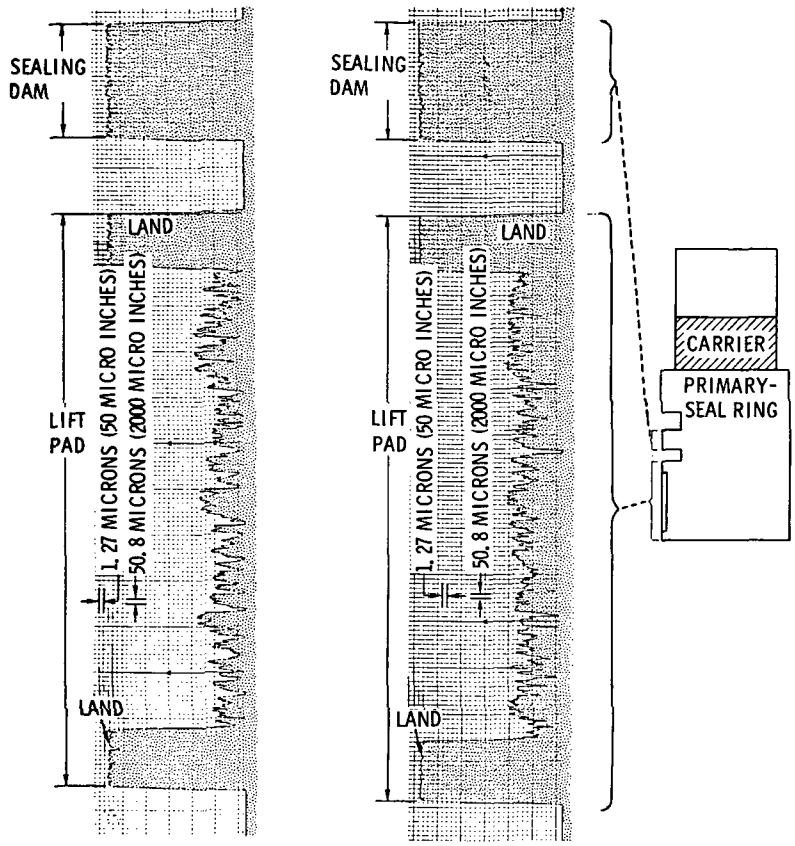

Figure 35. - Surface profile traces across self-acting pad and sealing dam before and after 38 hours of operation. Seal sliding speed, 122 to 183 meters per second (400 to 600 ft/sec); sealed pressure differential, 241 to 345 newtons per square centimeter (350 to 500 psi); sealed gas temperature, 811 K (1000° F).

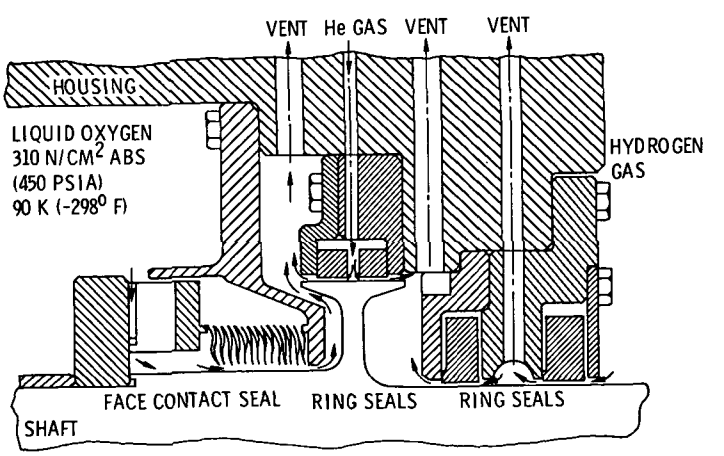

Figure 36. - Schematic of lox turbopump seal system, current practice.

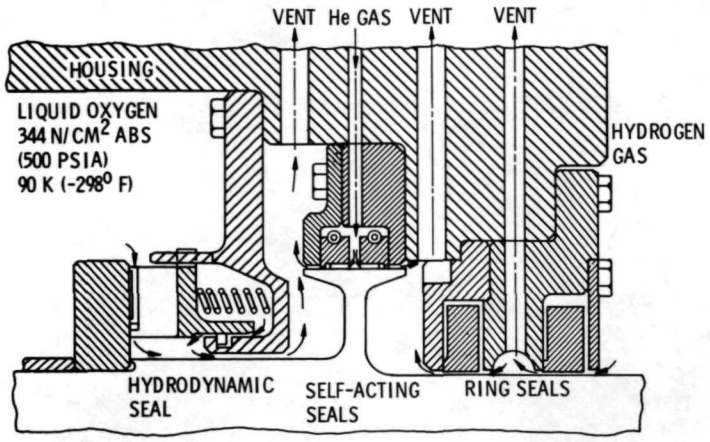

Figure 37. - Schematic of lox turbopump seal system under development.

Figure 38. - Circumferential seal self-acting type.